

## Mach Cones in a Coulomb Lattice and a Dusty Plasma

D. Samsonov, J. Goree,\* Z. W. Ma, and A. Bhattacharjee

*Department of Physics and Astronomy, The University of Iowa, Iowa City, Iowa 52242*

H. M. Thomas and G. E. Morfill

*Max Planck Institut für extraterrestrische Physik, 85740 Garching, Germany*

(Received 11 May 1999)

Mach cones, or V-shaped disturbances created by supersonic objects, have been detected in a two-dimensional Coulomb crystal. Electrically charged microspheres levitated in a glow-discharge plasma formed a dusty plasma, with particles arranged in a hexagonal lattice in a horizontal plane. Beneath this lattice plane, a sphere moved faster than the lattice sound speed. Mach cones were double, first compressive then rarefactive, due to the strongly coupled crystalline state. Molecular dynamics simulations using a Yukawa potential also show multiple Mach cones.

PACS numbers: 52.25.Zb

Mach cones are V-shaped disturbances produced by a supersonic object. They are familiar in gas dynamics [1], and, less commonly, they also occur in solid matter [2]. The cone's Mach angle is  $\mu = \sin^{-1}(1/M)$ , where  $M = v/c$  is the Mach number of an object moving at speed  $v$  through a medium with an acoustic speed  $c$ . This is different from a ship's wake in water, which is a transverse wave where  $\mu$  does not vary with  $v$ .

Here, we demonstrate the existence of Mach cones in a crystalline Coulomb lattice (Wigner crystal), i.e., a periodic structure of repulsive charges. Various physical systems, including colloidal spheres [3], can form a Wigner crystal. The experimental system we used was a strongly coupled dusty plasma. Dusty plasmas consist of electrons, ions, and small particles of solid matter [4–10], all held in a suspension analogous to a colloidal crystal [3]. The particles gain a large negative charge  $Q$ . Their repulsive interparticle potential is shielded by the electron-ion plasma, characterized by a Debye length  $\lambda_D$  [9]. The particle coupling is measured by the parameter  $\Gamma = Q^2/(4\pi\epsilon_0\Delta k_B T)$ , where  $\Delta$  is the distance between particles, and  $T$  is their kinetic temperature. Most plasmas are gaslike with  $\Gamma \ll 1$ . However, in experiments such as ours where  $\Gamma \gg 1$ , particles are said to be “strongly coupled,” and they are suspended in a highly ordered state [4,5,7,8].

The existence of Mach cones in dusty plasmas was predicted theoretically by Havnes *et al.* [6]. They also predicted that boulders moving through the dust of Saturn's rings should produce Mach cones.

We sustained an electron-ion plasma by applying a 13.56 MHz rf voltage to a horizontal Al electrode 230 mm in diameter, shown in Fig. 1. A grounded upper ring and the vacuum vessel served as the other electrode. The plasma was weakly ionized krypton at 0.05 mbar. Approximately  $10^4$  polymer spheres of diameter  $8.9 \pm 0.1 \mu\text{m}$  and density  $1.51 \text{ g/cm}^3$  were shaken into the plasma above the electrode. The spheres

were too massive to respond to the rf, which sustained the electron-ion plasma. The rf input power was 50 W, yielding a self-bias  $V_{dc} = -245 \text{ V}$  that levitated the negatively charged particles at  $z = 6.5 \text{ mm}$  above the lower electrode. In the radial direction, a gentle ambipolar electric field trapped the particles in a disk approximately

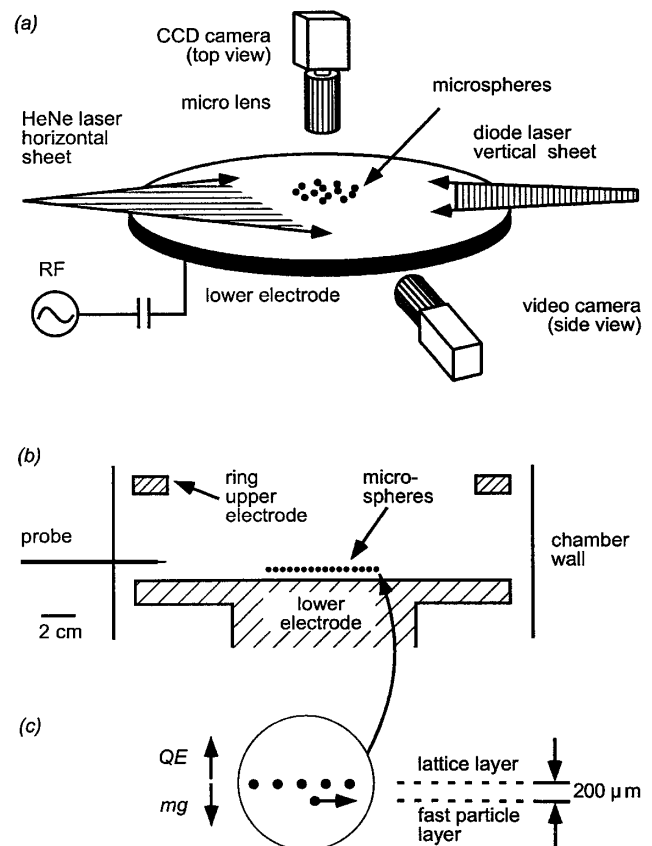


FIG. 1. (a) Sketch of apparatus. (b) Scale drawing of the electrodes. (c) Negatively charged microspheres are levitated above the lower electrode in a lattice; beneath it a few fast particles move horizontally.

40 mm in diameter. This disk, which we term the “lattice layer,” was a two-dimensional lattice, with a particle spacing  $\Delta = 256 \mu\text{m}$ , and very little particle motion.

Mach cones in the lattice layer were produced by charged particles moving in a second incomplete layer, 200  $\mu\text{m}$  beneath the lattice layer. This lower layer was populated by less than ten particles that moved rapidly, unlike particles in the lattice layer, in the horizontal direction. Presumably, they were accelerated by a horizontal electric force in the sheath, which we cannot explain. Sometimes they traversed the entire disk in a nearly straight line. They may have been single spheres or agglomerates of two or three.

To detect the microspheres, we illuminated them with a horizontal laser sheet and imaged them with a digital camera looking down through the ring’s opening. The camera operated at 50 frames/s. We observed many

cones. Several passed through the 1.37  $\text{cm}^2$  field of view each second. In this Letter, we analyze a representative example.

In each frame, the coordinates of each particle were identified, as in Fig. 2. Because we measure individual particle motion, rather than bulk parameters such as pressure, our experiment is different from observations of Mach cones in other systems.

Motion in the lattice layer was truly two-dimensional. Viewing from the side using a long-distance microscope with a video resolution of 2  $\mu\text{m}$ , we observed no vertical particle motion, even in the presence of cones.

There were not one, but two V-shaped Mach cones in our experiment. They are difficult to identify in the particle position map [Fig. 2(a)] but easily recognized in velocity maps. In Figs. 2(b) and 2(c), a fast particle moved in the 4 o’clock direction at 40 mm/s. The first

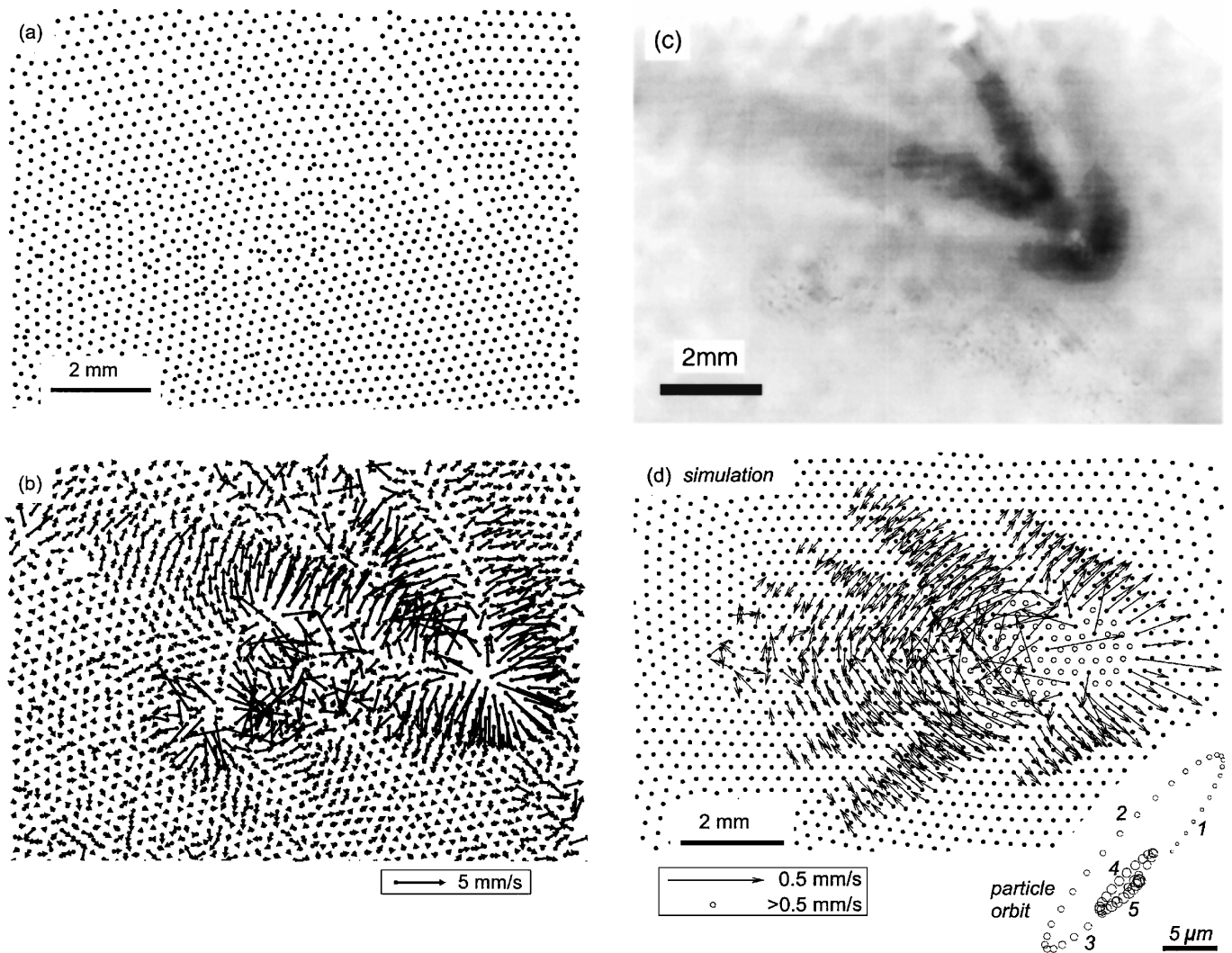


FIG. 2. (a) Particle positions in a single video frame, from the experiment. (b) Map of particle velocity  $\mathbf{v}$ , as computed from two consecutive frames. (c) Map of particle speed  $|\mathbf{v}|$ , computed from nine consecutive velocity maps by aligning them, averaging them, and calculating  $|\mathbf{v}|$ . (d) Molecular dynamics simulation. The inset shows the orbit of a particle located 0.77 mm above the centerline.

cone is a compression, which pushed particles forward. After the particles reached a maximum displacement of approximately  $0.5\Delta$ , they reversed direction, creating a second cone that was rarefactive, moving particles back toward their undisturbed positions.

This double cone does not occur in gas dynamics. We attribute it to the restoring force between nearest neighbors in a crystalline state. The second cone may be similar to the “unloading wave” that follows the initial compression of an elastic shock, in real solids [11].

The Mach angle was  $\mu = 33.5^\circ \pm 3^\circ$  for the first cone. The corresponding Mach number is  $M = 1.81 \pm 0.15$ . Using  $v = 40$  mm/s, which was measured separately, we obtain an acoustic speed  $c = 22 \pm 0.2$  mm/s. The second cone had a smaller angle of  $22^\circ \pm 2^\circ$ .

The vertex of the first cone is rounded rather than pointed. We attribute this to the finite size of the Debye sphere surrounding the fast particle. In gas dynamics, the vertex is rounded when the supersonic object is a sphere, and pointed when it is a needle.

To estimate  $\lambda_D$ , we diagnosed the plasma with a passively filtered Langmuir probe inserted  $z_0 = 11.6$  mm above the lower electrode. The electron temperature was  $T_{e0} = 0.9 \pm 0.1$  eV, and the plasma potential was  $V_{p0} = +11$  V (where the subscript 0 denotes a measurement at the probe height). Using the method of Ref. [12], we found  $\lambda_{D0} = (71.4_{-5}^{+12}) \mu\text{m}$ , yielding an ion density  $n_{i0} = (9.75_{-1.8}^{+0.2}) \times 10^9 \text{ cm}^{-3}$ , where the errors correspond to those in  $T_e$ . We expect plasma neutrality at the probe, but not at the particle height, where there is a large electric field. Moreover, due to an axial density profile,  $n_i$  at the particle height is reduced, compared to the probe height, by an unknown factor  $\beta$ ,  $n_i = n_{i0}/\beta$ . Estimating  $\beta = 3$  yields  $\lambda_D = 124 \mu\text{m}$ . In extreme limits  $\beta = 1$  and 10, we find  $\lambda_D = 67$  and  $264 \mu\text{m}$ , respectively.

We measured the vertical resonance frequency as 44.6 Hz, which allows a measurement of  $Q$ . Using the method of Ref. [5], with the charge density in the sheath at the particle height estimated as  $0.7en_i$ , yields  $2200 < -Q/e < 27\,000$ . The wide range of this result is due to the uncertainty in  $n_i$ . This is improved in an alternate method [13] that uses  $V_{dc}$ ,  $V_{p0}$ , and  $z$ , rather than the less precise  $n_i$ , yielding  $-Q/e = 23\,000$ . The accuracy of this value is limited primarily by the assumption of a parabolic potential inside the sheath.

The crystalline state of the 2D lattice in the experiment was verified by structural analysis methods [7] applied to an image without any Mach cones. Particle positions were used to compute the pair correlation function  $g(r)$ , while interparticle bonds were identified by Delaunay triangulation. Fitting  $g(r)$  in Fig. 3 yielded the interparticle separation  $\Delta = 256$  nm and a translation correlation length  $\xi = 4.3\Delta$ . The bonds had 85% sixfold particle coordination, with an orientation correlation length  $\xi_6 = 23\Delta$ . The large values of these structural parameters indicate that the lattice was primarily crystalline.

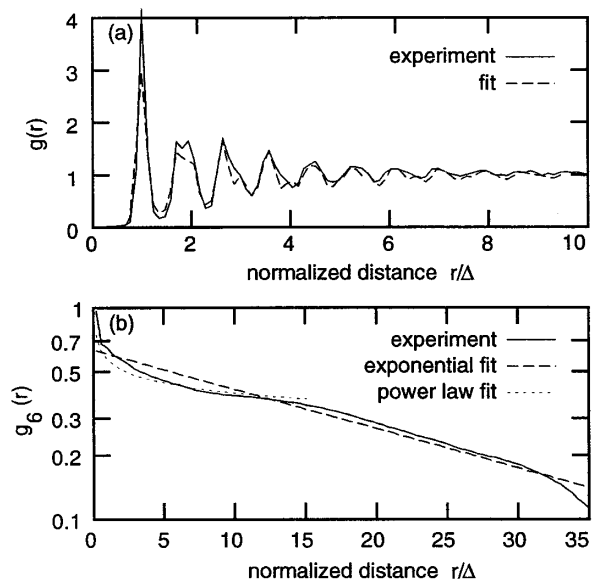


FIG. 3. Structural analysis from the experiment. (a) Pair correlation function. (b) Bond orientational correlation function. Distance is normalized by  $\Delta = 256 \mu\text{m}$ .

Because  $\Delta > \lambda_D$ , the particles in our two-dimensional hexagonal lattice interacted chiefly with their nearest six neighbors. Through the combination of short-range interparticle repulsion and the plasma’s radial electric field, the particles behaved as a planar hexagonal network of masses connected to nearest neighbors with springs. Particles were also subject to a gas drag force that is  $\propto v$ .

Like any crystal, a Coulomb lattice sustains both compressional (longitudinal) and shear (transverse) waves [3,14,15]. Because the former is significantly faster [3], it dominates the outer regions of the Mach cones. This mode is termed the dust-lattice wave (DLW) for  $\Delta > \lambda_D$  [10]. Its dispersion relation [8] is independent of the propagation direction in a 2D hexagonal lattice.

Here, we develop a method of using Mach cones to measure  $Q$ . For long wavelengths,  $\lambda > 2\pi\Delta$ , the DLW has only weak dispersion [3,10], and the acoustic speed  $c$  is proportional to  $Q$ . Neglecting damping and including only nearest-neighbor interactions, we find

$$Q_{\text{DLW}} = c \left[ \frac{\pi \epsilon_0 m \Delta \exp(\Delta/\lambda_D)}{A(1 + \Delta/\lambda_D) + B(\Delta/\lambda_D)^2} \right]^{1/2}. \quad (1)$$

The coefficient  $A = \frac{1}{2}$  for a 1D lattice and  $\frac{15}{32}$  for a 2D hexagonal lattice, while  $B = \frac{1}{4}$  and  $\frac{9}{32}$ , respectively. By measuring  $\mu$  and  $v$  to compute  $c$ , we use Eq. (1) to measure  $Q$ .

For our experiment, in a 2D lattice, we find  $13\,000 < -Q_{\text{DLW}}/e < 24\,000$ . The range is due to the uncertainty in  $\lambda_D$  at the particle layer. We find that  $Q_{\text{DLW}}$  is less sensitive to  $\lambda_D$  than  $Q_T$  is to  $n_i$ . As our best estimate, we assume  $\beta = 3$ , yielding  $Q_{\text{DLW}} = 15\,600e$ . Using this charge and  $T < 1200$  K, which we measured using a side-view camera, we find that  $\Gamma > 13\,000$ .

We performed a 2D molecular dynamics (MD) simulation of the experiment. A unique feature of strongly coupled dusty plasmas is that particle positions and velocities are measured in the experiment, just as they are in MD, thereby allowing a very direct comparison. The particle equation of motion  $m d^2 \mathbf{x} / dt^2 = -Q \nabla \varphi - \gamma d \mathbf{x} / dt$  was integrated for 2500 particles. The electric potential  $\varphi$  consisted of a parabolic potential to model the radial confinement from the plasma, plus a Yukawa interparticle repulsion:  $\varphi = -k \rho^2 / 2 \sum (Q_i / 4 \pi \epsilon_0 r_i) \exp(-r_i / \lambda_D)$ . Here,  $\rho$  is the distance from the central axis,  $r_i$  is the distance to particle  $i$ , and the sum is over all other particles. The experiments of Konopka *et al.* validated this potential in the horizontal plane [9]. We used parameters  $Q = 11\,270e$ ,  $\lambda_D = 200 \mu\text{m}$ ,  $m = 5.57 \times 10^{-10} \text{g}$ ,  $\gamma = 10 \text{s}^{-1}$  for Epstein drag with diffuse reflection [16], and we chose  $k = 1.1 \times 10^{-8} \text{g/s}^2$  to obtain  $\Delta = 250 \mu\text{m}$ . Particles seeded with random initial positions gradually settled into equilibrium positions as their kinetic energy was damped. After they formed a crystal, we introduced another particle moving 40 mm/s on a plane 200  $\mu\text{m}$  below the lattice layer, as in the experiment. We arbitrarily chose  $Q$  and  $\lambda_D$  for this fast particle to be the same as in the lattice layer, as these parameters were not measured experimentally.

The simulation results [Fig. 2(d)] reveal multiple Mach cones. The first cone is compressive, with  $\mu = 37^\circ$ , a rounded vertex, and tails of a finite length. There is not only a second cone, but a third and fourth as well. Within each of these secondary cones there is internal structure, with particles moving inward and then outward. The presence of more than one cone is due to a restoring force, as particles attempt to return to their original positions in the lattice, after the initial disturbance. This leads to a damped oscillation in particle position, as seen in the particle orbit plotted in the inset of Fig. 2(d). A similar ringing effect has been observed in seismology experiments and simulations [2].

In the simulations, we verified that  $\mu$  diminishes as  $v/c$  is increased. The simulation was also used to test the accuracy of Eq. (1) for measuring the particle charge. Computing  $c$  from the angle of the first cone, Eq. (1) yields a  $Q$  that is too large by 9% and 43%, for  $\Delta/\lambda_D = 2.1$  and 1.3, respectively. In the latter case, the nearest-neighbor assumption of Eq. (1) is not strongly satisfied.

In both the experiment and the simulation, we found that the tails of the cones have a finite length. They become shorter as the gas damping is increased. In the experiment, operating at a low gas pressure was a key requirement for observing any Mach cones at all. Wave dispersion could also contribute to the finite tail length.

While the experiment and simulation show agreement in many ways, there are differences. These include the

structure and amplitude of the cones. In the experiment, we cannot identify a third cone or internal structure in a cone. Either they are absent or they are not resolved in the presence of random motion. The reason for these discrepancies has not been determined. Another discrepancy is the amplitude of particle displacement, which was smaller in the simulation, perhaps due to choosing  $Q$  too small for the fast particle.

In another paper, we will report many Mach cone events, observed in experiments with various particle sizes and gases. In addition to velocity maps, such as Fig. 2, we will present number density maps. These will be used to measure conditions upstream and downstream of the propagating disturbance, allowing a comparison to the Hugoniot relations for shocks in solids. Defect maps will show that the lattice deformation is mainly elastic, rather than plastic. These experiments also verify that  $\mu$  decreases as with  $v/c$ .

We thank U. Konopka, S. Müller, R. Quinn, X. Wang, and M. Zuzic for their assistance. Work was supported in part by NASA and the National Science Foundation.

---

\*Electronic address:

- [1] H. W. Liepman and A. Roshko, *Elements of Gas Dynamics* (Wiley, New York, 1957).
- [2] N. Cheng, Z. Zhu, C. H. Cheng, and M. N. Toksöz, *Geophys. Prospect.* **42**, 303 (1994).
- [3] F. M. Peeters and Xiaoguang Wu, *Phys. Rev. A* **35**, 3109 (1987).
- [4] J. H. Chu and Lin I, *Phys. Rev. Lett.* **72**, 4009 (1994).
- [5] T. Trottenberg, A. Melzer, and A. Piel, *Plasma Sources Sci. Technol.* **4**, 450 (1995).
- [6] O. Havnes, T. Aslaksen, T. W. Hartquist, F. Li, F. Melandsø, G. E. Morfill, and T. Nitter, *J. Geophys. Res.* **100**, 1731 (1995).
- [7] R. A. Quinn, C. Cui, J. Goree, J. B. Pieper, H. Thomas, and G. E. Morfill, *Phys. Rev. E* **53**, R2049 (1996).
- [8] A. Homann, A. Melzer, R. Madanio, and A. Piel, *Phys. Lett. A* **242**, 173 (1998).
- [9] U. Konopka, L. Ratke, and H. M. Thomas, *Phys. Rev. Lett.* **79**, 1269 (1997); U. Konopka, G. E. Morfill, and L. Ratke (to be published).
- [10] N. Otani, A. Bhattacharjee, and X. Wang, *Phys. Plasmas* **6**, 409 (1999).
- [11] R. A. Graham, *Solids Under High-Pressure Shock Compression* (Springer-Verlag, New York, 1993), p. 19.
- [12] F. F. Chen, *Plasma Phys.* **7**, 47 (1965).
- [13] J. Goree (unpublished).
- [14] K. I. Golden, G. Kalman, and P. Wyns, *Phys. Rev. A* **46**, 3454 (1992).
- [15] P. K. Kaw and A. Sen, *Phys. Plasmas* **5**, 3552 (1998).
- [16] P. Epstein, *Phys. Rev.* **23**, 710 (1924).